

Agent Memory Below the Prompt: Persistent Q4 KV Cache for Multi-Agent LLM Inference on Edge Devices

Yakov Pyotr Shkolnikov
yshkolni@gmail.com

February 2026

Abstract

Multi-agent LLM systems on edge devices face a memory management problem: device RAM is too small to hold every agent’s KV cache simultaneously. On Apple M4 Pro with 10.2 GB of cache budget, only 3 agents fit at 8K context in FP16. A 10-agent workflow must constantly evict and reload caches. Without persistence, every eviction forces a full re-prefill through the model—15.7 seconds per agent at 4K context. We address this by persisting each agent’s KV cache to disk in 4-bit quantized format and reloading it directly into the attention layer, eliminating redundant $O(n)$ prefill computation via direct cache restoration. Because multi-agent systems naturally interleave (one agent generates while the next one loads), the reload latency (~ 500 ms) hides behind the previous agent’s decode phase. The system comprises three components: a block pool providing per-agent isolated Q4 KV caches in safetensors format, a BatchQuantizedKVCache for concurrent inference over multiple agents’ quantized caches, and cross-phase context injection that accumulates attention state across conversation phases without re-computation. Evaluated on three architectures (Gemma 3 12B, dense GQA, 48 layers; DeepSeek-Coder-V2-Lite 16B, MoE MLA, 27 layers; Llama 3.1 8B, dense GQA, 32 layers), cache restoration reduces time-to-first-token by up to $136\times$ (Gemma: $22\text{--}136\times$ at 4K–32K; DeepSeek: $11\text{--}76\times$ at 4K–32K; Llama: $24\text{--}111\times$ at 4K–16K; $3\text{--}10\times$ at 1K). Q4 quantization fits $4\times$ more agent contexts into fixed device memory than FP16; head-to-head benchmarking against vllm-mlx shows that FP16 prefix caching fails under realistic multi-agent memory pressure, requiring per-context server isolation at 8K+ and failing entirely at 16K even in isolation. Perplexity measured with actual Q4 KV caches shows -0.7% for Gemma (within measurement noise), $+2.8\%$ for Llama, and $+3.0\%$ for DeepSeek, consistent with prior Q4 quantization literature. The system handles all three architectures through a model-agnostic abstraction and exposes an OpenAI-compatible API. Open-source at <https://github.com/yshk-mxim/agent-memory>.

1 Introduction

Five agents, each holding 4,096 tokens of conversation history. On an Apple M4 Pro with 10.2 GB of cache budget, only 6 agents fit in FP16 at this context length, and only 3 at 8K. A 10-agent workflow cannot keep all agents in memory simultaneously. Every time the system switches to an evicted agent, it must re-prefill the full context through the model: 15.7 seconds per agent. The same problem occurs after a server restart, when all caches are lost: five agents \times 15.7 seconds = 78.5 seconds of dead time.

This is the cache management problem for multi-agent LLM inference on edge devices. Datacenter GPUs process tokens at 10,000+/second, making a 4K re-prefill a 400 ms annoyance. Apple Silicon processes them at roughly 260/second (Gemma 3 12B, M4 Pro). The gap is $40\times$, recurring on every agent switch throughout a session.

The problem is worse than slow prefill. Each agent needs its own attention context. Concatenating multiple agents’ histories into one long prompt introduces position bias: information in the middle of long sequences gets less attention than information at the start or end [1]. Separate KV caches per agent avoid this, but N agents with C tokens each require $N \times C$ tokens of cache memory on a device where RAM is soldered and fixed.

We eliminate re-prefill by persisting each agent’s KV cache to disk in 4-bit quantized format. Instead of freeing cache blocks for reuse on eviction (as vLLM [2] and SGLang [3] do) or holding them only in volatile RAM, we write them to SSD and reload when the agent resumes. Context restoration drops from 15.7 seconds to 577 ms (warm, disk)

or 719 ms (hot, memory) at 4K context on Gemma 3 12B. Head-to-head comparison with vllm-mlx shows Q4 warm-cache TTFT matches FP16 prefix-cache latency while surviving server restarts and memory pressure that cause FP16 cache failure (Section 4.4). Because multi-agent workflows naturally interleave—one agent generates while the next one loads—the reload latency hides behind decode. The system provides virtual memory for attention state: agents see unbounded context, while the block pool pages caches between memory and disk.

Contributions. (1) A persistent block pool giving each agent isolated, quantized KV cache surviving server restarts and device reboots, stored in safetensors format. (2) BatchQuantizedKVCache for concurrent Q4 inference over multiple agents’ caches, with an interleaved prefill+decode scheduler. (3) Cross-phase context injection that reuses cached attention state across conversation phases without re-computation. (4) Evaluation across three architecturally distinct models showing Q4 persistence fits $4\times$ more agents than FP16 with measured quality impact of -0.7% to $+3.0\%$ perplexity.

This is a systems paper. The individual techniques (KV cache quantization, disk persistence, batched inference) exist in prior work. Our contribution is their composition into a working system for multi-agent edge inference, with empirical characterization across three architecturally distinct models. The system exposes an OpenAI-compatible API, so any framework issuing chat completion requests can use persistent cache without modification.

2 Background

2.1 The Multi-Agent Memory Problem

LLM inference has two phases: prefill (process all input tokens in parallel, producing KV pairs for each attention layer) and decode (generate output tokens one at a time, attending to cached KV state). Prefill is compute-bound; decode is memory-bandwidth-bound.

Multi-agent systems compound the prefill cost. Each agent requires its own context because attention is quadratic in sequence length: a single 20K-token pass costs $25\times$ the attention of a 4K pass (quadratic: $(20K/4K)^2 = 25$). Five separate agents cost $5 \times (4K)^2$ total attention, while concatenating them into one 20K prompt costs $(20K)^2$ — $5\times$ more expensive. Concatenation also exposes answers to position bias [1]: agents in the middle of the concatenated context receive less attention weight. Separate contexts are necessary for unbiased multi-agent inference.

Separate contexts mean separate KV caches. A 5-agent system needs 5 independent caches. Real agentic workflows can involve 5–20+ agents: AutoGen teams, CrewAI crews, and debate architectures each assign specialized roles [4], and each role requires independent conversational state. SagaLLM identifies “context loss” over extended multi-step workflows as a fundamental limitation of current multi-agent systems [5].

On a datacenter GPU, keeping 20 caches in memory is routine. On an edge device with 24 GB of fixed RAM, keeping 5 caches requires lifecycle management: which caches to keep hot, which to persist to disk, and when to reload. Without persistence, every agent cold-starts from scratch on every request.

2.2 Edge Device Constraints

Server GPUs have 80–192 GB of HBM, with multi-GPU nodes reaching terabytes. Edge devices ship with soldered DRAM. A 24 GB MacBook Pro will always have 24 GB. Table 1 shows current edge-class hardware.

The RTX 5090 has 1,792 GB/s bandwidth to its 32 GB VRAM, but spilling KV cache to host RAM drops to 64 GB/s (PCIe 5.0), a $28\times$ cliff. Unified memory devices avoid this penalty but face fixed total capacity. The M4 Pro’s internal NVMe reads at up to 7 GB/s, which enables sub-second cache reloads for multi-MB KV states.

On our test device (M4 Pro, 24 GB), the memory budget is 24 GB – 6.8 GB weights – 7 GB OS/system \approx 10.2 GB for KV caches. This constrains both the number of concurrent agents and the maximum context length per agent (Section 3.2).

Local inference avoids transmitting conversation history to external servers. Under GDPR (Art. 44–49), transferring personal data outside the EU requires legal basis and transfer impact assessments; under HIPAA (45 CFR 164.312), transmitting protected health information requires technical safeguards and business associate agreements. On-device inference sidesteps this. Per-agent cache isolation also prevents the prompt reconstruction attacks demonstrated by PROMPTPEEK [6], where shared KV caches enable 99% recovery of other users’ prompts. This isolation maps onto compliance requirements: each agent’s safetensors file constitutes an independently addressable data record

Table 1: Edge device memory and bandwidth. Unified memory devices share RAM between CPU and GPU. Discrete GPUs (RTX) have separate VRAM; KV cache offload to host RAM drops to PCIe bandwidth.

Device	Mem (GB)	BW (GB/s)	SSD (GB/s)	Type
M4 Pro (MacBook Pro)	24	273	~7	Unified
M4 Max (MacBook)	128	546	7	Unified
DGX Spark	128	273	11	Unified
RTX 5090 (VRAM)	32	1792	64*	Discrete
RTX 4090 (VRAM)	24	1008	32*	Discrete
iPhone 17 Pro [†]	12	77	2	Unified

*PCIe host-device bandwidth for KV cache offload.

[†]Projected specifications; device not yet released.

supporting role-based access control, audit-trail separation, and targeted erasure under GDPR Article 17. Encryption at rest for safetensors files provides an additional technical safeguard under HIPAA’s Security Rule. The tradeoff: operating within fixed device memory.

2.3 Interactivity and TTFT

Response latency determines whether interactive agents feel responsive. Nielsen’s thresholds [7] identify 100 ms as instantaneous, 1 s as acceptable, and 10 s as the limit before users disengage. In 2023, Nielsen reported that no AI system tested met the 1 s threshold for complex queries [8].

For short multi-turn agent responses (50–200 tokens at ~50 tok/s = 1–4 s decode), prefill dominates perceived latency. At 4K context on Gemma 3, cold prefill is 15.7 s. Adding 3 s decode gives 18.7 s total, of which 84% is prefill. At shorter outputs (50 tokens, 1 s decode), prefill is 94% of latency.

RAG does not solve this because it re-retrieves text chunks and re-runs prefill over them on every request. Prefill accounts for 95.5% of RAG inference time [9]. RAGCache [10] mitigates this by caching intermediate KV states across RAG queries, but targets datacenter deployments.

KV cache persistence eliminates the $O(n)$ prefill, replacing it with I/O-bound cache reload. At 4K context, Gemma warm-cache TTFT is 577 ms. This crosses Nielsen’s 1 s threshold into acceptable territory.

3 System Design

3.1 Block Pool with Per-Agent Isolation

The block pool partitions KV cache into fixed-size blocks of 256 tokens, organized by agent ID. Each agent’s cache consists of AgentBlocks (a per-layer mapping from layer index to a list of KVBlock instances) where each KVBlock stores per-layer key/value tensors in Q4 format (uint32 packed data + bfloat16 scales/biases). A ModelCacheSpec captures architectural parameters (layer count, KV head count, head dimensions, quantization settings) without model-specific logic.

Each agent’s cache is independently addressable. Server restart, model swap, or concurrent inference over multiple agents cannot corrupt or mix cache state. The block pool enforces namespace isolation at the data structure level.

3.2 Q4 Quantization Pipeline

KV cache flows through the system in 4-bit quantized format at every stage:

1. **Disk:** uint32 packed weights + bfloat16 scales/biases in safetensors format
2. **Memory:** Same format, loaded via native safetensors I/O (`mx.load()`)
3. **Attention:** `mlx-lm’s quantized_scaled_dot_product_attention()` operates directly on Q4 tensors

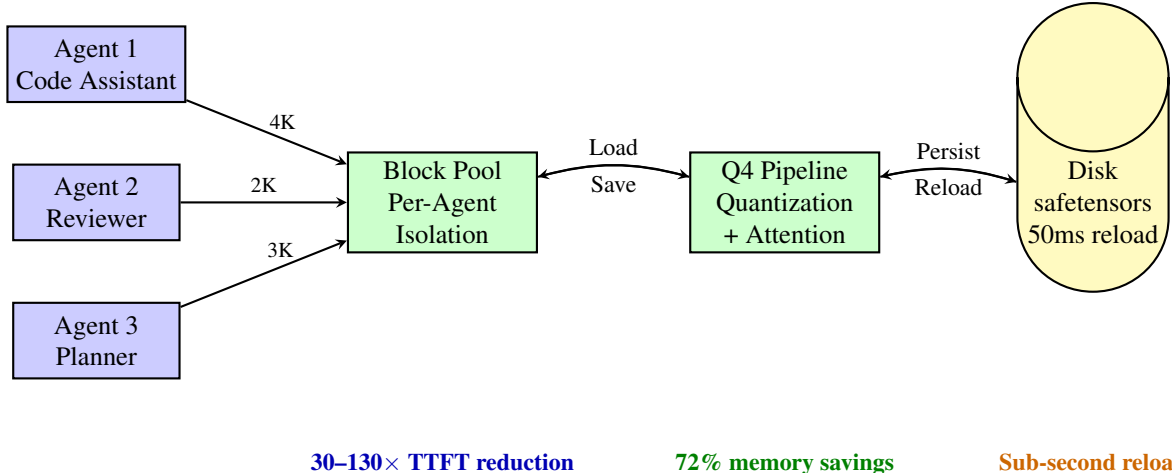


Figure 1: System architecture. Multiple agents maintain isolated KV caches in a persistent block pool. The Q4 pipeline quantizes cache data on save and operates directly on quantized tensors during attention. Disk persistence enables sub-100ms reload (warm) vs seconds of re-prefill (cold).

Table 2: Agent capacity on M4 Pro (10.2 GB cache budget). Gemma 3 12B, 48 layers, 8 KV heads, head dim 256.

Context	FP16/agent	Q4/agent	FP16 fits	Q4 fits
4K	1.5 GB	0.42 GB	6	24
8K	3.0 GB	0.84 GB	3	12
16K	6.0 GB	1.7 GB	1	6
32K	12.0 GB	3.4 GB	0	3

For a layer with h KV heads, head dimension d , sequence length n , and group size $g=64$: FP16 stores $4hdn$ bytes (K+V, 2 bytes per element). Q4 packs each element into 4 bits and adds a bfloat16 scale and bias per group of g elements, totaling $hdn(1 + 8/g)$ bytes. The ratio $Q4/FP16 = (1 + 8/g)/4 = 0.281$ for $g=64$, yielding 72% memory reduction per layer regardless of model dimensions.

Why Q4, not FP16. On the M4 Pro with 10.2 GB cache budget, Table 2 shows the capacity difference. FP16 KV for Gemma 3 at 4K context costs $2 \times 8 \times 256 \times 4096 \times 2 \times 48 = 1,536$ MB per agent. Q4 at the 0.281 ratio costs 432 MB. At 8K context with 5 agents, FP16 requires 15 GB (1.5× the budget). Q4 uses 4.2 GB, leaving 6 GB free. Full calculations for all three models appear in Appendix D.

3.3 Prefix Matching

Standard prefix-caching systems [2; 3] match by comparing token IDs. This breaks when BPE tokenization is context-dependent: the same text produces different token sequences depending on surrounding tokens. We compare raw prompt text at the character level. Given a cached text and a new prompt, the system returns EXACT (identical), EXTEND (new prompt starts with cached text), or DIVERGE (insufficient overlap). A 50% common-prefix threshold determines reuse eligibility. In practice, multi-phase agent workflows produce monotonically growing prompts (EXTEND match), so partial reuse is rarely exercised.

3.4 Batched Quantized Inference

MLX upstream libraries (mlx-lm v0.30) do not provide batched inference over quantized KV caches. We implement BatchQuantizedKVCache with three operations: **merge** (left-pad shorter sequences, stack along batch dimension), **update_and_fetch** (compute attention over the unified batch, update with new KV pairs), and **extract** (split back into per-agent caches, remove padding).

A ConcurrentScheduler alternates between agents during prefill (configurable chunk size, default 512 tokens) and interleaves decode steps, adapting the iteration-level scheduling principle introduced by Orca [11] for quantized caches on edge devices. This provides uniform latency distribution, per-token SSE streaming during batched generation, and peak memory bounded by chunk size rather than total batch size.

Concurrency model. MLX is not thread-safe (GitHub issues #2067, #2133, #3078). Concurrent `mx.eval()` calls from different threads cause Metal assertion failures. All MLX inference runs on a single scheduler thread. An RLock (`mlx_io_lock`) serializes cross-thread operations (cache saves to disk). This provides time-sliced cooperative concurrency rather than true parallelism. Batched inference is effective because the GPU processes merged batch tensors in a single forward pass: two agents’ decode steps execute as one Metal kernel dispatch.

3.5 Cross-Phase Context Injection

Multi-phase agent workflows (negotiation, interrogation, debate) traditionally re-compute context from scratch at each phase. We use **working memory** to refer to the subset of KV cache state that accumulates across conversational phases and is available for reuse without re-computation—analogueous to a workspace that persists across task switches. We treat KV cache as persistent working memory: Phase 1 processes the initial prompt and saves cache; Phase 2 loads the Phase 1 cache, constructs Phase 2 prompt so its prefix matches Phase 1 text, extends with new context (EXTEND match), and generates; Phase N accumulates cache across all phases.

Prompts follow a structured template that enforces monotonic cache extension. Each phase appends rather than replaces, so the cached prefix always matches.

3.6 Architectural Coverage

The system handles two architecturally distinct model families (GQA and MLA) through the ModelCacheSpec abstraction.

Gemma 3 12B uses dense layers with grouped-query attention (GQA) [12]. Of its 48 attention layers, 8 use global attention and 40 use sliding-window attention (window size 1024). GQA maps 8 KV heads to 16 query heads ($n_{rep}=2$). The KV cache is symmetric: keys and values both have head dimension 256. For batched GQA, we reshape queries to 5D (B, n_{kv}, n_{rep}, L, D) and expand the attention mask with an extra dimension for broadcast compatibility within the fused Q4 attention kernel. Chunked prefill generates sliding-window masks for the 40 windowed layers and global causal masks for the 8 global layers.

DeepSeek-Coder-V2-Lite 16B [13] uses Mixture-of-Experts (MoE) with Multi-Latent Attention (MLA). All 27 layers use global attention. MLA compresses keys and values into low-rank latent representations, producing asymmetric cache dimensions: $K=192$ (128 nope + 64 rope), $V=128$. We added a `v_head_dim` field to ModelCacheSpec and detect MLA at runtime via the `qk_nope_head_dim` attribute on attention modules. MoE routing creates intermediate tensors during forward passes, requiring a larger memory budget (4096 MB vs Gemma’s 2048 MB).

All three models use the same block pool, Q4 pipeline, and BatchQuantizedKVCache. The abstraction boundary is ModelCacheSpec. Everything above it is model-agnostic. A detailed architectural comparison appears in Appendix H.

4 Evaluation

4.1 Setup

Hardware. Apple MacBook Pro M4 Pro (MX2E3LL/A), 24 GB unified LPDDR5X, 273 GB/s bandwidth.

Models. Gemma 3 12B Instruct (48 attention layers, 8 KV heads, head dim 256, GQA with 16 query heads). DeepSeek-Coder-V2-Lite 16B Instruct (27 layers, 16 KV heads, $K=192/V=128$, MLA). Llama 3.1 8B Instruct (32 layers, 8 KV heads, head dim 128, standard GQA). All at Q4 weights with Q4 KV cache.

Methodology. Each configuration is measured 6 times; we report medians. Temperature 0.0 (greedy decoding, deterministic output). Output length fixed at 64 tokens. 11–240s adaptive cooldown between runs (thermal-aware, monitoring TPS recovery to baseline). TTFT: wall-clock time from request submission to first streamed token. Sys-tem TPS (SysTPS): total tokens generated across all concurrent agents divided by wall-clock seconds; for batch=2, SysTPS counts both agents’ tokens. Per-agent TPS = SysTPS / batch size. The full matrix targets 6 context lengths

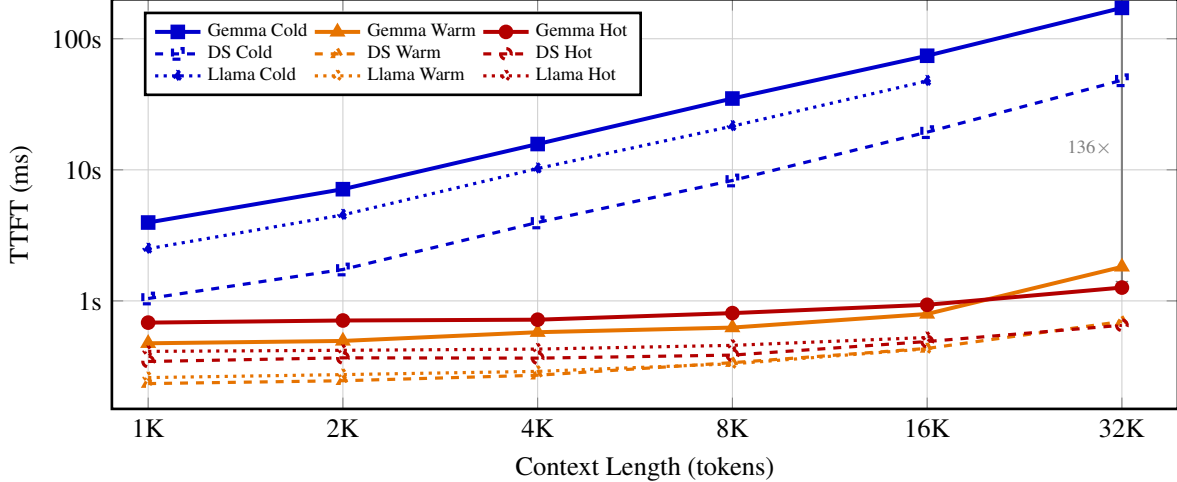


Figure 2: TTFT scaling across cache states for all three models (Gemma solid, DeepSeek dashed, Llama dotted). Cold prefill scales linearly with context length. Hot and warm caches reduce TTFT by up to $136\times$ at 32K (Gemma) and $111\times$ at 16K (Llama), with sub-second reload up to 16K context. Llama 3.1 8B falls between Gemma and DeepSeek in cold prefill, but achieves the highest warm speedups ($111\times$ at 16K) due to its smaller 8B parameter count enabling fast cache reload relative to cold.

Table 3: TTFT (ms) by cache state. Streaming, batch=1, median of 6 passes.

Model	Cache	1K	2K	4K	8K	16K	32K
Gemma 3	Cold	3964	7119	15736	35009	74219	172096
	Warm	475	495	577	626	795	1819
	Hot	683	709	719	807	934	1264
DeepSeek	Cold	1043	1737	3970	8296	19396	47315
	Warm	234	246	271	338	434	633
	Hot	345	368	366	386	490	624
Llama 3.1	Cold	2500	4530	10235	21536	47629	—
	Warm	260	274	290	331	431	—
	Hot	412	420	429	458	526	—

$\times 3$ cache states $\times 2$ batch sizes $\times 2$ streaming modes per model. Gemma: 394 measurements (1K–32K; 32K batch=2 excluded, 2 hot non-streaming missing). DeepSeek: 378 measurements (1K–32K; 32K batch=1 only, 3 passes). Llama: 360 measurements (1K–16K). Total: 1,132 individual measurements plus 36 staggered arrival tests, all passing quality checks. Corpus: 151 KB diverse Wikipedia text (~ 37.7 K tokens) drawn from articles on Bayesian inference, central limit theorem, Markov chains, Monte Carlo methods, and six other topics (full list in the repository at [benchmarks/corpus/](#)).

4.2 TTFT Scaling

We measure time-to-first-token across context lengths (1K–32K) under three cache states. **Cold**: no cached data, full prefill. **Warm**: KV cache persisted to disk, reloaded from safetensors. **Hot**: KV cache resident in memory.

Cold TTFT scales linearly with context (Table 3, Figure 2). Gemma at 32K takes 172 seconds (2.87 minutes). DeepSeek is $3.6\times$ faster at 32K (fewer layers, smaller hidden dimensions); Llama 3.1 8B falls between them at 47.6 s for 16K (dense GQA, 32 layers). All three models exhibit $O(n)$ scaling.

Warm TTFT is nearly flat. Disk I/O plus cache restoration dominates, and these costs grow slowly with cache size. Gemma warm ranges from 475–1819 ms across 1K–32K. DeepSeek warm ranges from 234–633 ms (1K–32K). Llama warm ranges from 260–431 ms (1K–16K). The speedup over cold grows with context: at 16K, Gemma warm is $93\times$

Table 4: Single vs concurrent throughput (non-streaming, median of 6 passes). Single: batch=1. Concurrent: batch=2, SysTPS = total tokens/second across both agents.

Context	Cache	Gemma 3		DeepSeek		Llama 3.1	
		SysTPS	Per	SysTPS	Per	SysTPS	Per
1K	Cold	10.4	5.2	35.5	17.8	16.6	8.3
1K	Warm	22.6	11.2	63.0	31.5	37.8	18.9
1K	Hot	22.1	11.1	73.1	36.6	38.3	19.1
4K	Cold	3.5	1.8	13.5	6.8	5.9	2.9
4K	Warm	19.6	9.9	52.6	26.3	34.5	17.2
4K	Hot	19.3	9.6	61.6	30.8	43.3	21.6
16K	Cold	0.8	0.4	3.1	1.6	1.3	0.7
16K	Warm	11.9	5.9	27.9	14.0	26.1	13.1
16K	Hot	14.9	7.5	31.9	16.0	36.5	18.3

faster, DeepSeek warm is $45\times$ faster, Llama warm is $111\times$ faster. Llama achieves the highest speedups because its 8B parameter count means fast warm reload relative to its already-moderate cold prefill.

Hot TTFT is also nearly flat and close to warm. Gemma hot ranges from 683–1264 ms, DeepSeek hot from 345–624 ms (1K–32K), Llama hot from 412–526 ms. At 16K, Gemma hot is $79\times$ faster than cold, DeepSeek hot is $40\times$ faster, Llama hot is $91\times$ faster. The gap between warm and hot is small (within $2\times$) because disk I/O on the internal SSD takes only 5–80 ms.

A consistent artifact appears at short contexts (1K–8K), where Gemma’s and Llama’s hot TTFT exceeds warm by 40–55% (e.g., Gemma 1K: 683 ms hot vs 475 ms warm, reproduced across all 6 passes with zero crossovers). The warm path reads the cache file via a single `mx.load()` call that triggers an optimized sequential I/O path in MLX. The hot path performs per-layer hash lookups, validation checks, and scattered memory accesses across the block pool’s in-memory data structures. At short contexts the cache file is small (a few MB), so sequential disk I/O completes faster than the scattered memory access pattern. At 32K where the cache file exceeds 3 GB, disk I/O dominates and hot wins (1264 ms vs 1819 ms).

Measurement variability. Each configuration is measured 6 times with adaptive thermal cooldown between passes. Cold TTFT has coefficient of variation (CV) under 2.5% across all configurations—prefill computation is deterministic, with only system-level timing jitter. Warm TTFT shows CV of 1–9% (I/O timing varies with system load). Hot TTFT shows CV of 1–14% (one DeepSeek 1K outlier at 457 ms vs median 345 ms; excluding it, CV < 7%). Decode TPS is stable at CV < 3% across all configurations. All reported values are medians of 6 passes.

4.3 Batched Throughput

Table 4 shows system throughput when serving two concurrent agents. Cold batched throughput is low because prefill dominates. At 16K, Gemma achieves only 0.8 system TPS (both agents stuck in prefill). Warm and hot caches skip prefill, so system TPS depends only on batched decode speed.

DeepSeek is $2\text{--}3\times$ faster than Gemma in batched throughput. At 4K warm, DeepSeek reaches 52.6 system TPS (26.3 per agent) vs Gemma’s 19.6 (9.9 per agent). DeepSeek’s MoE architecture activates 6 of 64 routed experts (plus 2 shared) per token, reducing compute per decode step despite the larger parameter count. Llama falls between them: 34.5 system TPS at 4K warm (17.2 per agent), consistent with its smaller 8B parameter count and standard GQA architecture.

The warm-to-hot gap is small for all three models. Disk reload latency is amortized over the generation and does not bottleneck sustained throughput.

4.4 Comparison with vllm-mlx

Table 5 compares TTFT against vllm-mlx [14] using Llama 3.1 8B, where vllm-mlx’s `--continuous-batching` mode correctly enables prefix caching. We chose Llama rather than Gemma for this comparison because vllm-mlx v0.2.6 misclassifies Gemma 3 as a multimodal model, routing it through a non-functional MLLM batching path that

Table 5: Head-to-head TTFT comparison: agent-memory (Q4 KV cache, disk-persistent) vs vllm-mlx [14] (FP16 KV cache, volatile). Llama 3.1 8B Q4 weights, streaming, batch=1, median of 3 passes. “Warm” = agent-memory Q4 cache loaded from SSD. “Prefix” = vllm-mlx FP16 prefix cache hit (in-memory only). “Restart” = server killed and restarted, then same prompt re-sent. vllm-mlx run with `--continuous-batching --cache-memory-percent 0.40` (9.6 GB of 24 GB UMA for FP16 prefix cache). Benchmark structured as cold→prefix per context to prevent FP16 cache eviction (Section 4.4).

Context	agent-memory (Q4 KV)			vllm-mlx (FP16 KV)		
	Cold	Warm	Restart	Cold	Prefix	Restart
1K	2,500	260	260	2,289	273	2,262
2K	4,530	274	274	2,204	204	4,134
4K	10,235	290	290	4,394	290	8,079
8K	21,536	331	331	9,472 [†]	244 [†]	—
16K	47,629	431	431	37,935 [†]	371 [‡]	—

[†]Isolated run (fresh server, single context). FP16 eviction prevented multi-context benchmarking.

[‡]Median of 2/3 passes; third evicted even in isolation. “—” = no data (eviction or OOM).

disables prefix caching entirely (GitHub issue #54). Both systems share the same underlying mlx-lm inference engine, tokenizer, and Metal attention kernels; the comparison isolates the cache strategy: FP16 in-memory prefix cache (vllm-mlx) vs Q4 disk-persistent cache (agent-memory).

FP16 KV cache requires per-context benchmarking. vllm-mlx stores KV cache in FP16, consuming ~ 128 KB per token for Llama 8B. Our initial benchmark ran all five context lengths cold (1K through 16K, 3 passes each) before testing prefix-cached TTFT. This caused prefix cache eviction: the accumulated FP16 state exceeded the 9.6 GB cache budget, and prefix-cached tests failed starting at 4K context. We restructured the benchmark to test cold→prefix-cached per context, but even then 8K prefix caching failed on pass 3 (after 1K–4K contexts had consumed cache capacity) and 16K failed entirely. Running 8K and 16K in *complete isolation* (dedicated server, single context length) confirmed prefix caching works: 244 ms at 8K (3/3 OK), 216 ms at 16K (2/3 OK; pass 3 failed even alone). This restructuring was unnecessary for agent-memory, whose Q4 KV cache stores the same tokens in ~ 2.9 GB.

The interleaved failure scenario (five contexts of different lengths: 1K, 2K, 4K, 8K, 16K) represents the *minimum* multi-agent workload: a single agent per context length. FP16 prefix caching cannot support even this imbalanced configuration, let alone multiple agents per context length.

Cold prefill: vllm-mlx is faster. Without any cache, vllm-mlx is $\sim 2.3\times$ faster at 4K (4,394 ms vs 10,235 ms). To isolate the cause, we ran agent-memory with FP16 KV cache (disabling Q4 quantization): cold TTFT at 4K was 9,976 ms, only 259 ms faster than Q4, confirming that Q4 quantization adds $<3\%$ overhead. The remaining ~ 5.6 s gap is agent-memory’s orchestration layer (coordination service, block pool allocation, agent ID lookup, scheduler queue management). vllm-mlx also exhibits a ~ 2 s fixed floor at 1K–2K (2,289 ms and 2,204 ms respectively), likely reflecting Metal shader precompilation that is amortized differently: vllm-mlx compiles shaders during model loading, while agent-memory’s mlx-lm path compiles lazily on the first forward pass for each new sequence shape. Cold overhead is a one-time cost per agent per server session; every subsequent request uses warm cache, and with disk persistence the warm cache survives restarts.

Q4 warm cache matches FP16 prefix latency. When prefix cache hits, vllm-mlx achieves low TTFT (273 ms at 1K, 204 ms at 2K, 290 ms at 4K). Agent-memory’s warm Q4 disk reload converges to the same range (260 ms at 1K, 274 ms at 2K, 290 ms at 4K). Running agent-memory with FP16 KV cache confirms this is not coincidental: FP16 warm TTFT is 254 ms at 1K, 260 ms at 2K, and 348 ms at 4K. At 4K, the Q4 path (290 ms) is *faster* than FP16 (348 ms) because reading a $4\times$ smaller file from SSD outweighs the dequantization cost. On UMA hardware where SSD reads at ~ 7 GB/s, smaller data wins. Q4 and FP16 caching differ in deployment properties, not speed: vllm-mlx’s FP16 prefix cache is volatile (lost on restart, eviction, or memory pressure) and consumes $4\times$ more memory per cached token. Agent-memory’s Q4 cache persists to disk, surviving all three.

Persistence. After a full server restart, agent-memory’s cache survives on disk. TTFT remains at warm-cache levels. vllm-mlx’s FP16 prefix cache is volatile: restart discards all cached state, reverting to full cold prefill.

Memory density is required for agentic workloads. In multi-agent scenarios, memory pressure is an assured outcome: N agents \times C context tokens of FP16 KV state grows linearly. On a 24 GB device with ~ 16 GB free after model loading, FP16 fits ~ 7 agents at 16K context; Q4 fits ~ 30 . Our benchmark results make this concrete:

Table 6: Component contributions. Each row compares the system with vs without one component, holding others constant.

Component	Metric	With	Without	Effect
Persistence	TTFT (ms), Gemma 4K	577	15736	27×
Q4 vs FP16	Agents at 8K	12	3	4.0×
Batching	SysTPS, Gemma 1K warm	22.6	11.2*	2.0×
Cross-phase	TTFT (ms), Phase 5	1705	3292	1.9×

*Per-agent TPS = SysTPS/2. The 2.0× is definitional (system vs per-agent), not a measured throughput gain over batch=1.

vllm-mlx failed to produce any output at 16K context (both cold and prefix-cached) due to FP16 memory exhaustion, and prefix-cached tests at 8K succeeded on only 2 of 3 passes. Even with the per-context benchmark restructuring, accumulated FP16 state from earlier contexts evicted later entries. Agent-memory completed all measurements at all context lengths up to 32K. Neither vllm-mlx nor the GPU vLLM supports quantized KV cache (vLLM offers FP8 KV on CUDA only; an INT4 KV RFC has been stalled since 2025). llama.cpp [15] supports Q4 KV cache via its GGML backend but uses a different compute framework than MLX, and its per-slot save/restore requires manual API calls with no automatic multi-agent management.

Fused Q4 attention. Agent-memory patches mlx-lm’s attention dispatch with a fused quantized scaled dot-product attention kernel that wraps Q4 KV cache operations in `mx.compile(shapeless=True)` with correct GQA mask broadcasting. vllm-mlx delegates entirely to mlx-lm’s stock attention path (its `attention.py` is a compatibility shim, noting “attention is handled internally by mlx-lm”). Both systems use FP16 weights with the same mlx-lm decode loop; vllm-mlx achieves 49–55 tok/s on Llama 8B (batch=1) vs agent-memory’s 39–46 tok/s. The ~15% gap reflects agent-memory’s orchestration overhead (block pool, scheduler, coordination service) on each decode step, not attention kernel differences. The fused Q4 kernel’s contribution is enabling quantized cache decode at all. Without it, mlx-lm’s stock attention crashes on GQA mask broadcasting for batch>1 (Section 4.5).

The systems address complementary problems: vllm-mlx optimizes throughput via continuous batching with FP16 prefix caching; agent-memory optimizes latency and capacity via persistent Q4 cache. A combined approach (continuous batching with disk-backed Q4 cache) could capture both benefits.

4.5 Ablation Analysis

Table 6 isolates each component’s contribution. All numbers come from existing benchmark data (Tables 3–7) or analytical calculations (Table 2).

Persistence contributes the largest single improvement (27× TTFT reduction at 4K) by eliminating re-computation entirely. The other components improve what happens after the cache is loaded.

Q4 quantization matters for capacity rather than speed. At 8K context, FP16 fits 3 agents in 10.2 GB; Q4 fits 12. For a 5-agent workflow, FP16 cannot fit all agents while Q4 has room for execution overhead.

Batching serves two agents concurrently with a per-agent throughput cost. At 1K warm, batch=1 produces 13.2 per-agent TPS (Gemma); batch=2 produces 22.6 system TPS but only 11.2 per agent, a 15% per-agent reduction. The trade-off is worthwhile: Agent B begins generating immediately rather than waiting in a queue for Agent A to finish, reducing B’s wall-clock latency despite the lower per-agent throughput.

Cross-phase injection accumulates benefit over conversation phases. Phase 1 shows no improvement (both modes cold-start). By Phase 5, the persistent cache has grown across 4 prior phases, and reload is 1.9× faster than re-prefill. In longer workflows (10+ phases), the accumulated savings are expected to grow.

4.6 Multi-Phase Cache Persistence

Multi-agent workflows often span several phases (interrogation rounds, debate stages, collaborative drafts). Without persistent cache, each phase re-prefills every agent from scratch. We tested a 5-phase prisoner’s dilemma scenario

Table 7: Measured per-phase average TTFT (ms). Cold: caches cleared each phase. Persistent: caches accumulate. 25 turns total per run.

Phase	Gemma 3			DeepSeek		
	Cold	Pers	×	Cold	Pers	×
1: Interrogation A	1136	1079	1.1	477	460	1.0
2: Interrogation B	1119	976	1.1	465	430	1.1
3: The Yard	1648	1019	1.6	532	474	1.1
4: Final Reckoning	2195	1250	1.8	664	542	1.2
5: Verdict	3292	1705	1.9	874	649	1.3
Total wall (s)	72.9	56.1	1.3	33.6	27.8	1.2

Table 8: Wikipedia routing TTFT (ms) by phase. 10 experts, 5 queries, 3 repeated. Articles are 3K words (~4K tokens) each.

Phase	Gemma 3		DeepSeek	
	TTFT	Quality	TTFT	Quality
1: Priming (cold)	20514	8/10	5140	3/10
2: Queries (warm)	847	8/10	396	4/10
3: Repeated (hot)	860	3/3	424	2/3
Warm/cold speedup	24.2×		13.0×	
Hot/cold speedup	23.9×		12.1×	

with 4 agents (3 permanent, 1 ephemeral) and 25 total conversational turns.

Scenario structure. A warden interrogates two suspects (Marco, Danny) separately (Phases 1–2), suspects confer in the yard (Phase 3), all meet for a final reckoning (Phase 4), and an analyst renders a verdict (Phase 5). Permanent agents use `persistent_cache_prefix`, enabling EXTEND-match cache hits.

Phase 1 shows no benefit (both modes cold-start). By Phase 5, persistent mode reduces TTFT by 1.9× (Gemma) and 1.3× (DeepSeek). Total wall time drops 23% (Gemma) and 17% (DeepSeek). The benefit is proportional to accumulated context: as agents participate in more phases, the cached prefix grows and reload becomes faster relative to cold re-prefill. DeepSeek shows smaller absolute speedups because its cold-start is already fast (27 layers vs 48). A timeline visualization of cache state transitions appears in Appendix H.

4.7 Multi-Agent Routing

Information-retrieval workflows route queries to domain-expert agents. We tested a Wikipedia routing benchmark with 10 expert agents, each primed with a 2–4K token article on a statistics topic (Bayesian inference, regression analysis, hypothesis testing, etc.).

Three-phase protocol. Phase 1 (priming): each expert processes its article, cold-starting at 2–4K context. Phase 2 (cross-topic queries): 5 questions route to 2–3 relevant experts each; experts’ caches are warm/hot from priming. Phase 3 (repeated queries): 3 experts re-queried with additional context; caches are hot.

Quality evaluation. Each response is checked for non-emptiness, sufficient length (≥ 50 tokens), absence of repetition loops, and keyword relevance to the source article.

Table 8 shows measured results. Cold priming averages 20.5 s (Gemma) and 5.1 s (DeepSeek) per expert at ~4K token context. After priming, warm-cache queries drop to 847 ms (Gemma, 24.2× faster) and 396 ms (DeepSeek, 13.0×). Per-expert breakdown: the largest cold TTFT is 28 s (Gemma, 3K-word article), reduced to 761 ms warm. Quality passes range from 80% (Gemma Phase 2) to 30% (DeepSeek Phase 1); these scores measure structural quality (keyword overlap, minimum length), not factual accuracy. DeepSeek-Coder is optimized for code tasks, not general knowledge retrieval; the low quality scores reflect model capability, not caching artifacts. A routing diagram appears in Appendix H.

Table 9: Perplexity with actual Q4 KV caches. FP16 baseline uses standard KV cache; Q4 uses the production QuantizedKVCache (group size 64). 7,935 tokens, 512-token windows, 256-token stride.

Model	FP16 PPL	Q4 PPL	Δ PPL	$\Delta\%$
Gemma 3 12B	14.40	14.30	-0.10	-0.7
DeepSeek-V2-Lite 16B	6.26	6.45	+0.19	+3.0
Llama 3.1 8B	4.28	4.40	+0.12	+2.8

4.8 Q4 Cache Quality

We measure the quality impact of Q4 KV cache quantization using actual `QuantizedKVCache` objects from the production code path. For each model, we evaluate perplexity on a local WikiText-2 corpus using 512-token sliding windows with 256-token stride, processing 7,935 tokens total. Quantization error propagates through all attention layers, matching real inference conditions.

Table 9 shows measured results. Gemma 3 shows a -0.10 PPL change (-0.7%), within measurement noise (Q4 cannot improve over FP16 in principle; the negative sign reflects evaluation variance). This is consistent with the negligible degradation reported by KIVI [16] and KVQuant [17] at 4 bits. DeepSeek shows a $+0.19$ PPL increase ($+3.0\%$), small in absolute terms but larger than Gemma’s. Llama 3.1 shows $+0.12$ PPL ($+2.8\%$), falling between Gemma and DeepSeek, consistent with its standard GQA architecture.

The divergence between models likely reflects architectural differences in how quantization error distributes. Gemma’s GQA uses symmetric KV dimensions ($K=V=256$ per head), providing redundancy across the 8 KV heads that absorbs quantization noise. Llama’s GQA uses smaller symmetric dimensions ($K=V=128$ per head), with less redundancy per head, yielding moderate degradation ($+2.8\%$). DeepSeek’s MLA compresses keys and values into low-rank latent representations with asymmetric dimensions ($K=192, V=128$). The compressed latent space has less redundancy to absorb 4-bit rounding error, and the asymmetric K/V dimensions mean quantization affects keys and values differently. GEAR [18] introduces a low-rank matrix plus sparse correction to reduce quantization error in KV caches; our uniform Q4 pipeline trades this error correction for simplicity and portability. Prior Q4 KV cache work [16; 17; 19] reports <0.1 PPL degradation on standard GQA models; our Gemma result is consistent, while Llama and DeepSeek show that smaller head dimensions and asymmetric architectures incur measurable but tolerable Q4 degradation.

Limitations of this measurement. The evaluation uses a local WikiText-2 corpus, not the standard benchmark split. The 512-token evaluation windows are shorter than Gemma’s sliding-window attention ($\text{window}=1024$), so the measurement does not exercise cross-window attention dynamics. We do not report confidence intervals. Longer-context evaluation and per-layer sensitivity analysis are future work.

5 Discussion

5.1 Infrastructure Layer for Agentic Systems

This system occupies the infrastructure layer beneath agentic frameworks. AutoGen [20], CrewAI, and LangGraph manage agent logic: role assignment, turn-taking, tool use. Our system manages agent memory, deciding which caches to keep hot, which to spill to disk, and when to reload. The cache lifecycle (persist, reload, evict) is transparent to the application layer. Any framework that issues OpenAI-compatible chat completion requests can use persistent cache without modification.

The capacity constraint makes cache swapping the common case. At 8K context with Q4, only 12 agents fit in 10.2 GB (Table 2). A 20-agent workflow (representative of multi-crew architectures) keeps 12 caches hot and constantly pages the remaining 8 between disk and memory. Without persistence, each page-in costs a full re-*prefill* (15.7 s at 4K). With Q4 disk persistence, page-in costs ~ 500 ms of I/O.

Latency hiding follows from multi-agent structure. In a 5-agent round-robin, while Agent A generates (1–3 s for 50–100 tokens at ~ 50 tok/s), Agent B’s cache loads from disk (~ 500 ms at 7 GB/s). The I/O is fully hidden: decode takes longer than reload. The interleaved scheduler already implements this for *prefill* chunks. In principle, only $1/N$ of reload latency falls on the critical path, where N is the number of active agents. For $N=5$, cache reload could run concurrently with generation 80% of the time. This is analogous to virtual memory paging but for attention state: the

Table 10: Context restoration approaches for multi-turn agents.

	RAG	KV Persist	Msg Pass
Restore cost	$O(n)$ prefill	$O(n)$ I/O	$O(n)$ rebuild
Stores	Text chunks	Attn state	Structured msgs
Scope	External KB	Conv. history	Inter-agent
Model-specific	No	Yes	No
Hardware	Vector DB	SSD/RAM	Network

Table 11: Feature comparison with related systems. Pool: per-agent cache isolation. BQ4: batched Q4 inference. WM: cross-phase KV persistence. Edge: UMA device support. Multi: dense + MoE architectures. Disk: persistent cache survives restart.

System	Pool	BQ4	WM	Edge	Disk
vLLM [2]	Paged	FP8 [†]	No	No	No
SGLang [3]	Radix	No	No	No	No
vllm-mlx [14]	Prefix	No	No	Yes	No
llama.cpp [15]	Slot	Q4 [‡]	No	Yes	Slot [§]
mlx-engine [21]	No	Q8	No	Yes	No
KVSwap [22]	No	No	No	Yes	No
KVCOMM [23]	No	No	Share	No	No
KVFlow [24]	Prefix	No	Flow	No	No
MemArt [25]	Reuse	No	Yes	No	No
Continuum [26]	TTL	No	TTL	No	No
CommVQ [27]	No	2bit	No	No	No
LMCache [28]	Chunk	No	No	No	Tier
This work	Agent	Q4	Yes	Yes	Yes

[†]FP8 KV cache (CUDA only). [‡]Q4/Q8 via `--cache-type-k/v` (GGML, not MLX).

[§]Manual per-slot save/restore via API; no automatic multi-agent management.

^{||}KV quantization limited to non-sliding-window models prior to v0.15.1.

block pool acts as a page table, SSD serves as swap, and multi-agent interleaving provides the temporal slack that hides page faults. The $1/N$ projection has not been measured end-to-end; the staggered arrival results (Appendix F) provide partial validation for $N=2$.

5.2 Persistent Cache vs RAG vs Message Passing

Persistent KV cache occupies a distinct design point from RAG and message passing (Table 10). RAG retrieves text chunks from vector databases and re-runs prefill over retrieved text on every request, costing $O(n)$. KV cache persistence reloads computed attention state via I/O, avoiding recomputation. Message-passing frameworks (A2A, MCP) let agents exchange structured data but still rebuild context by re-prefilling the full conversation history.

These are complementary. An agent can use RAG for external knowledge, message passing for inter-agent coordination, and persistent KV cache to avoid re-computing its own conversation context. The persistent cache contribution is latency, not accuracy: both re-prefill and cache reload produce the same attention state (modulo Q4 quantization error), but reload is 11–136× faster at 4K–32K (Gemma: 22–136×; DeepSeek: 11–76×; Llama: 24–111×).

5.3 Comparison with Related Systems

Table 11 positions this system. Per-agent persistent Q4 storage on edge devices with batched quantized inference and working memory semantics has not, to our knowledge, been addressed by prior work. The closest feature-wise is llama.cpp [15], which supports both quantized KV cache (`--cache-type-k q4_0`) and per-slot cache save/restore via its `/slot/save` API. However, llama.cpp uses the GGML backend (not MLX), requires manual API calls for

each save/restore operation, and provides no automatic multi-agent cache management, LRU eviction, or block pool isolation. LM Studio’s `mlx-engine` [21] (closed-source application, open-source engine) adds in-memory KV cache quantization on MLX, but does not persist cache to disk and encountered type-mismatch errors with sliding-window models (e.g., Gemma 3) at prompts exceeding the window size prior to release 0.15.1. `vllm-mlx` [14] provides MLX-native prefix caching with FP16 KV cache but no quantized KV storage or disk persistence. MemArt [25] introduces KV reuse blocks with working memory but targets datacenters and lacks a Q4 pipeline. No prior system provides `BatchQuantizedKVCache` for concurrent Q4 inference across multiple agents’ persistent caches on edge devices.

5.4 Why Unified Memory Matters

The viability of KV cache persistence depends on the ratio of storage bandwidth to memory bandwidth. On unified memory devices, the internal SSD reads at ~ 7 GB/s into a 273 GB/s memory system—an SSD-to-UMA ratio of $\sim 2.6\%$. On discrete GPU systems, spilling KV cache from VRAM to host RAM drops from 1,792 GB/s (RTX 5090 HBM) to ~ 64 GB/s (PCIe 5.0 $\times 16$), a PCIe-to-VRAM ratio of $\sim 3.5\%$ (~ 24 – $28\times$ cliff in practice; theoretical peak is $28\times$). Although the ratios are comparable, the critical difference is that UMA devices access SSD-loaded data at full memory bandwidth once loaded, whereas discrete GPUs face the PCIe bottleneck on every cache miss. This makes KV cache persistence architecturally viable on UMA but less attractive for discrete GPU deployments where the offload penalty recurs at inference time.

5.5 Portability

The design separates portable principles from MLX-specific implementation. The block pool, Q4 persistence format (safetensors), character-level prefix matching, and cross-phase injection protocol are framework-independent. A PyTorch port would replace MLX’s quantized attention with equivalent kernels (e.g., TensorRT-LLM FP8 or CUTLASS INT4) and `mx.save_safetensors` with `safetensors.torch`.

The non-portable aspects are MLX’s lazy evaluation model (requiring explicit `mx.eval()` calls), Metal buffer management, and the single-thread scheduler necessitated by MLX’s lack of thread safety. On CUDA, PyTorch’s eager execution and CUDA stream synchronization allow different concurrency models.

5.6 Limitations

Single device. All agents share one device. Multi-device extension would require cache transfer over Thunderbolt or network interconnects.

Q4 quality impact. Section 4.8 measures perplexity with actual Q4 KV caches, showing -0.10 PPL (-0.7%) for Gemma, $+0.12$ PPL ($+2.8\%$) for Llama, and $+0.19$ PPL ($+3.0\%$) for DeepSeek. These measurements use 512-token evaluation windows, which do not exercise Gemma’s sliding-window attention (`window=1024`). Longer-context evaluation and per-layer sensitivity analysis are future work.

Three models tested. We validate on Gemma 3 12B (dense GQA with hybrid attention), DeepSeek-Coder-V2-Lite 16B (MoE with MLA), and Llama 3.1 8B (dense standard GQA). While these span the major attention architectures, testing on larger models (70B+) is left to future hardware.

Model-specific caches. KV caches are tied to the model that produced them. A Gemma 3 cache cannot be used by a different model or a different quantization of the same model. Model updates invalidate all cached state. RAG text chunks survive model swaps; KV caches do not.

Fixed output length. All measurements use 64-token output. Longer outputs would reduce the relative TTFT speedup since decode time (unaffected by caching) grows. At 512 tokens output, the TTFT savings remain identical but constitute a smaller fraction of end-to-end latency.

No working memory quality metric. Cross-phase context injection eliminates re-prefill latency but does not change the information available to the model. Both persistent cache and re-prefill produce equivalent context (modulo Q4 rounding). The contribution is speed, not accuracy.

Cache deletion semantics. Cache deletion is file deletion: removing an agent’s `safetensors` file erases all persisted attention state for that agent. The block pool maintains a registry mapping agent IDs to cache files, enabling targeted erasure. Whether quantized attention state constitutes personal data under GDPR’s broad definition depends on whether the original input contained PII; the system does not currently inspect cache content for PII classification.

6 Related Work

KV cache management. vLLM [2] partitions KV cache into paged blocks ($2\text{--}4\times$ throughput). SGLang [3] uses a radix tree for prefix reuse ($5\times$ throughput). Both free cache blocks after request completion (with LRU prefix reuse) and target datacenter GPUs. LMCache [28] adds multi-engine persistent KV storage with tiered offloading (GPU \rightarrow CPU \rightarrow SSD) for enterprise deployments. Continuum [26] assigns TTL values to cached KV entries for multi-turn scheduling (up to $3.66\times$ delay reduction, datacenter). DistServe [29] disaggregates prefill and decode across GPUs; Sarathi-Serve [30] uses chunked prefill with stall-free scheduling on the same GPU. Both target datacenter-scale throughput.

vllm-mlx [14], developed concurrently with our system (December 2025–February 2026), provides in-memory prefix caching with SHA-256 deduplication and continuous batching on MLX ($21\text{--}87\%$ higher throughput than llama.cpp on Apple Silicon). Our system addresses an orthogonal problem: cross-session persistence via disk-backed safetensors cache, enabling warm-start TTFT after server restarts, cache eviction, or device sleep/wake cycles. We provide a head-to-head comparison in Section 4.4.

Offloading and scheduling lineage. FlexGen [31] introduced GPU-CPU-disk offloading with compressed KV cache for throughput-oriented generation on a single GPU. Our work adds per-agent isolation, cross-session persistence via safetensors, and targets edge UMA devices rather than datacenter GPUs. Orca [11] introduced iteration-level scheduling (continuous batching), which decouples individual requests from batch boundaries. Our scheduler adapts this principle for quantized caches on edge devices, interleaving chunked prefill with batched decode within MLX’s single-thread constraint.

KV cache compression. KIVI [16] quantizes keys per-channel and values per-token at 2 bits ($2.6\times$ memory reduction). KVQuant [17] adds per-layer sensitivity analysis supporting up to 1M context on a single A100-80GB (10M on 8-GPU). CommVQ [27] achieves 87.5% reduction at 2 bits using vector quantization commutative with RoPE. QuantSpec [19] uses hierarchical Q4 KV cache for speculative decoding, validating 4-bit cache utility for speculative decoding. We use 4-bit quantization with an end-to-end Q4 pipeline from disk through attention. Prior quantization work operates on in-memory single-session caches; we extend Q4 to persistent disk storage with cross-session reuse.

Agent memory. EM-LLM [32] organizes tokens into episodic events using Bayesian surprise (30.5% improvement over the top-ranked retriever (NV-Embed-v2) on LongBench). A-MEM [33] organizes agent memories in Zettelkasten-style note networks. MemArt [25] introduces KV-cache-centric memory with reusable blocks ($91\text{--}135\times$ prefill reduction). We focus on per-agent isolation and cross-phase persistence rather than external knowledge injection. MemArt targets datacenters and lacks Q4 quantization or disk persistence.

Multi-agent KV systems. KVCOMM [23] enables cross-context KV sharing for multi-agent systems ($7.8\times$ speedup, $>70\%$ cache reuse). KVFlow [24] uses workflow-aware cache eviction ($2.19\times$ concurrent speedup). Both target datacenter deployments. PROMPTPEEK [6] shows that shared KV caches enable 99% prompt reconstruction attacks, which motivates per-agent isolation.

Edge inference. KVSwap [22] offloads KV cache to disk on edge devices for long-context inference. Kelle [34] co-designs KV cache with eDRAM for custom edge accelerators ($3.9\times$ speedup) but requires specialized hardware. Rajesh et al. [35] benchmark local LLM inference on Apple Silicon without addressing multi-agent cache management. Krul [36] uses dynamic cross-layer KV sharing for efficient multi-turn state restoration but does not address persistent disk caching.

llama.cpp [15] supports quantized KV cache (Q4, Q8) and per-slot save/restore to disk via its server API, but uses the GGML backend, requires manual save/restore calls per slot, and provides no automatic multi-agent orchestration, block pool, or LRU eviction. LM Studio’s mlx-engine [21] is the closest MLX-native alternative, offering in-memory KV cache quantization; however, it is a closed-source application (with an open-source engine component), does not persist cache to disk, and KV quantization was incompatible with sliding-window attention models prior to release 0.15.1.

7 Conclusion

Persistent Q4 KV cache turns agent context restoration from a compute-bound $O(n)$ prefill into an I/O-bound cache reload. On Gemma 3 12B at 32K context, hot cache reduces TTFT from 172 seconds to 1.3 seconds ($136\times$). On DeepSeek-Coder-V2-Lite at 32K, from 47.3 seconds to 624 ms ($76\times$). On Llama 3.1 8B at 16K, from 47.6 seconds to

526 ms (91×). Warm disk reload achieves 95×, 75×, and 111× respectively.

On edge devices with fixed memory, Q4 KV cache is essential: FP16 fits only 3 agents at 8K context on 24 GB, while Q4 fits 12. At longer contexts (16K+), FP16 cannot fit even a single multi-agent workflow. The measured quality impact is -0.10 to $+0.19$ PPL across all three models (Section 4.8). Batched serving reaches 23 system TPS (Gemma), 63 system TPS (DeepSeek), and 38 system TPS (Llama) with two warm-cache agents at 1K context.

Two multi-agent scenarios validate the design. A 5-phase interrogation shows 1.9× TTFT reduction in later phases from cross-phase persistence (23% total wall-time reduction). A 10-expert routing benchmark shows 24× TTFT reduction when querying cached experts.

At 4K context, cloud inference (H100 at $\sim 15,000$ tok/s + 100 ms network) achieves ~ 370 ms TTFT. On-device warm cache achieves ~ 577 ms (Gemma). On-device inference trades raw speed for deployment properties: no network dependency, no per-token cost, and data sovereignty.

Multi-device cache transfer, adaptive quantization bit-width (2-bit via RotateKV or CommVQ techniques), and porting to CUDA/RTX for discrete GPU edge devices are directions for future work.

Open-source at <https://github.com/yshk-mxim/agent-memory>.

References

- [1] Nelson F. Liu, Kevin Lin, John Hewitt, Ashwin Paranjape, Michele Bevilacqua, Fabio Petroni, and Percy Liang. Lost in the middle: How language models use long contexts. *Transactions of the Association for Computational Linguistics*, 12:157–173, 2024.
- [2] Woosuk Kwon, Zhuohan Li, Siyuan Zhuang, Ying Sheng, Lianmin Zheng, Cody Hao Yu, Joseph E. Gonzalez, Hao Zhang, and Ion Stoica. Efficient memory management for large language model serving with pagedattention. In *Proceedings of the 29th Symposium on Operating Systems Principles*, pages 611–626, 2023.
- [3] Lianmin Zheng, Liangsheng Yin, Zhiqiang Xie, Jeff Huang, Chuyue Sun, Cody Hao Yu, Shiyi Cao, Christos Kozyrakis, Ion Stoica, Joseph E. Gonzalez, Clark Barrett, and Ying Sheng. Sglang: Efficient execution of structured language model programs. In *Advances in Neural Information Processing Systems*, 2024.
- [4] Taicheng Guo, Xiuying Chen, Yaqi Wang, Ruidi Chang, Shichao Pei, Nitesh V. Chawla, Olaf Wiest, and Xiangliang Zhang. Large language model based multi-agents: A survey of progress and challenges. In *International Joint Conference on Artificial Intelligence*, pages 8048–8057, 2024.
- [5] Edward Y. Chang and Longling Geng. Sagallm: Context management, validation, and transaction guarantees for multi-agent llm planning. *Proceedings of the VLDB Endowment*, 18(12):4874–4886, 2025.
- [6] Guanlong Wu, Zheng Zhang, Yao Zhang, Weili Wang, Jianyu Niu, Ye Wu, and Yinqian Zhang. I know what you asked: Prompt leakage via kv-cache sharing in multi-tenant llm serving. In *Network and Distributed System Security Symposium (NDSS)*, 2025.
- [7] Jakob Nielsen. *Usability Engineering*. Academic Press, San Diego, CA, 1993. Chapter 5: Response Times: The 3 Important Limits (0.1s, 1.0s, 10s).
- [8] Jakob Nielsen. The need for speed in AI. Jakob Nielsen on UX (Substack), 2023. Published August 2, 2023. Argues no AI system tested meets the 1-second response time threshold.
- [9] Jiahao Wang, Weiyu Xie, Mingxing Zhang, Boxing Zhang, Jianwei Dong, Yuening Zhu, Chen Lin, Jinqi Tang, Yaochen Han, Zhiyuan Ai, Xianglin Chen, Yongwei Wu, and Congfeng Jiang. From prefix cache to fusion rag cache: Accelerating llm inference in retrieval-augmented generation. *arXiv preprint arXiv:2601.12904*, 2026. Reports prefill = 95.53% of RAG inference time.
- [10] Chao Jin, Zili Zhang, Xuanlin Jiang, Fangyue Liu, Xin Liu, Xuanzhe Liu, and Xin Jin. Ragcache: Efficient knowledge caching for retrieval-augmented generation. *ACM Transactions on Computer Systems*, 2024.
- [11] Gyeong-In Yu, Joo Seong Jeong, Geon-Woo Kim, Soojeong Kim, and Byung-Gon Chun. Orca: A distributed serving system for Transformer-Based generative models. In *16th USENIX Symposium on Operating Systems Design and Implementation (OSDI 22)*, pages 521–538. USENIX Association, 2022.

- [12] Joshua Ainslie, James Lee-Thorp, Michiel de Jong, Yury Zemlyanskiy, Federico Lebron, and Sumit Sanghai. GQA: Training generalized multi-query transformer models from multi-head checkpoints. In *Proceedings of the 2023 Conference on Empirical Methods in Natural Language Processing*, pages 4895–4901. Association for Computational Linguistics, 2023.
- [13] DeepSeek-AI. DeepSeek-V2: A strong, economical, and efficient mixture-of-experts language model. *arXiv preprint arXiv:2405.04434*, 2024. URL <https://arxiv.org/abs/2405.04434>.
- [14] Wayner Barrios. Native llm and mllm inference at scale on apple silicon. *arXiv preprint arXiv:2601.19139*, 2026.
- [15] Georgi Gerganov and contributors. llama.cpp: Llm inference in C/C++, 2023. URL <https://github.com/ggml-org/llama.cpp>. Supports quantized KV cache (Q4_0, Q8_0) via `--cache-type-k/v` and per-slot cache save/restore via `/slot/save` API.
- [16] Zirui Liu, Jiayi Yuan, Hongye Jin, Shaochen Zhong, Zhaozhuo Xu, Vladimir Braverman, Beidi Chen, and Xia Hu. Kivi: A tuning-free asymmetric 2bit quantization for kv cache. In *Proceedings of the 41st International Conference on Machine Learning*, volume 235 of *Proceedings of Machine Learning Research*, pages 32332–32344. PMLR, 2024.
- [17] Coleman Hooper, Sehoon Kim, Hiva Mohammadzadeh, Michael W. Mahoney, Yakun Sophia Shao, Kurt Keutzer, and Amir Gholami. Kvquant: Towards 10 million context length llm inference with kv cache quantization. In *Advances in Neural Information Processing Systems*, volume 37, 2024.
- [18] Hao Kang, Qingru Zhang, Souvik Kundu, Geonhwa Jeong, Zaoxing Liu, Tushar Krishna, and Tuo Zhao. GEAR: An efficient error reduction framework for KV cache compression in LLM inference. In *Proceedings of the 4th NeurIPS Efficient Natural Language and Speech Processing Workshop*, volume 262 of *Proceedings of Machine Learning Research*, pages 305–321. PMLR, 2024.
- [19] Rishabh Tiwari, Haocheng Xi, Aditya Tomar, Coleman Hooper, Sehoon Kim, Maxwell Horton, Mahyar Najibi, Michael W. Mahoney, Kurt Keutzer, and Amir Gholami. Quantspec: Self-speculative decoding with hierarchical quantized kv cache. In *Proceedings of the 42nd International Conference on Machine Learning*, PMLR, 2025.
- [20] Qingyun Wu, Gagan Bansal, Jieyu Zhang, Yiran Wu, Beibin Li, Erkang Zhu, Li Jiang, Xiaoyun Zhang, Shaokun Zhang, Jiale Liu, Ahmed Hassan Awadallah, Ryen W. White, Doug Burger, and Chi Wang. Autogen: Enabling next-gen LLM applications via multi-agent conversations. In *Conference on Language Modeling*, 2024.
- [21] LM Studio. mlx-engine: MLX inference engine for LM Studio, 2024. URL <https://github.com/lmstudio-ai/mlx-engine>. MLX-native inference with KV cache quantization support (PR #77); sliding-window models require release $\geq 0.15.1$.
- [22] Huawei Zhang, Chunwei Xia, and Zheng Wang. Kvsnap: Disk-aware kv cache offloading for long-context on-device inference. *arXiv preprint arXiv:2511.11907*, 2025.
- [23] Hancheng Ye, Zhengqi Gao, Mingyuan Ma, Qinsi Wang, Yuzhe Fu, Ming-Yu Chung, Yueqian Lin, Zhijian Liu, Jianyi Zhang, Danyang Zhuo, and Yiran Chen. Kvcomm: Online cross-context kv-cache communication for efficient llm-based multi-agent systems. In *Advances in Neural Information Processing Systems*, 2025. URL <https://arxiv.org/abs/2510.12872>.
- [24] Zaifeng Pan, Ajjkumar Patel, Zhengding Hu, Yipeng Shen, Yue Guan, Wan-Lu Li, Lianhui Qin, Yida Wang, and Yufei Ding. Kvflow: Efficient prefix caching for accelerating llm-based multi-agent workflows. In *Advances in Neural Information Processing Systems*, 2025. URL <https://arxiv.org/abs/2507.07400>.
- [25] Yuan Zeng, Pengfei Zuo, Min Lyu, Xingkun Yang, Huatao Wu, Yinlong Xu, and Zhou Yu. Kvcache-centric memory for llm agents. In *International Conference on Learning Representations*, 2026. URL <https://openreview.net/forum?id=YolJJOZOGhI>. Submitted to ICLR 2026.

- [26] Hanchen Li, Qiuyang Mang, Runyuan He, Qizheng Zhang, Huanzhi Mao, Xiaokun Chen, Hangrui Zhou, Alvin Cheung, Joseph Gonzalez, and Ion Stoica. Continuum: Efficient and robust multi-turn llm agent scheduling with kv cache time-to-live. *arXiv preprint arXiv:2511.02230*, 2025. URL <https://arxiv.org/abs/2511.02230>.
- [27] Junyan Li, Yang Zhang, Muhammad Yusuf Hassan, Talha Chafekar, Tianle Cai, Zhile Ren, Pengsheng Guo, Foroozan Karimzadeh, Colorado Reed, Chong Wang, and Chuang Gan. Commvq: Commutative vector quantization for kv cache compression. In *Proceedings of the 42nd International Conference on Machine Learning*, PMLR, 2025.
- [28] Yuhan Liu, Yihua Cheng, Jiayi Yao, Yuwei An, Xiaokun Chen, Shaoting Feng, Yuyang Huang, Samuel Shen, Rui Zhang, Kuntai Du, and Junchen Jiang. LMCache: An efficient KV cache layer for enterprise-scale LLM inference. https://lmcache.ai/tech_report.pdf, 2025.
- [29] Yinmin Zhong, Shengyu Liu, Junda Chen, Jianbo Hu, Yibo Zhu, Xuanzhe Liu, Xin Jin, and Hao Zhang. Dist-serve: Disaggregating prefill and decoding for goodput-optimized large language model serving. In *18th USENIX Symposium on Operating Systems Design and Implementation*, 2024.
- [30] Amey Agrawal, Nitin Kedia, Ashish Panwar, Jayashree Mohan, Nipun Kwatra, Bhargav S. Gulavani, Alexey Tumanov, and Ramachandran Ramjee. Taming throughput-latency tradeoff in llm inference with sarathi-serve. In *18th USENIX Symposium on Operating Systems Design and Implementation*, 2024.
- [31] Ying Sheng, Lianmin Zheng, Binhang Yuan, Zhuohan Li, Max Ryabinin, Daniel Y. Fu, Zhiqiang Xie, Beidi Chen, Clark W. Barrett, Joseph E. Gonzalez, Percy Liang, Christopher Ré, Ion Stoica, and Ce Zhang. High-throughput generative inference of large language models with a single GPU. In *Proceedings of the 40th International Conference on Machine Learning*, 2023. URL <https://arxiv.org/abs/2303.06865>.
- [32] Zafeirios Fountas, Martin A. Benfeghoul, Adnan Oomerjee, Fenia Christopoulou, Gerasimos Lampouras, Haitham Bou-Ammar, and Jun Wang. Em-llm: Human-inspired episodic memory for infinite context llms. In *International Conference on Learning Representations*, 2025.
- [33] Wujiang Xu, Zujie Liang, Kai Mei, Hang Gao, Juntao Tan, and Yongfeng Zhang. A-mem: Agentic memory for llm agents. In *Advances in Neural Information Processing Systems*, 2025. URL <https://arxiv.org/abs/2502.12110>.
- [34] Tianhua Xia and Sai Qian Zhang. Kelle: Co-design kv caching and edram for efficient llm serving in edge computing. In *IEEE/ACM International Symposium on Microarchitecture*, 2025. URL <https://dl.acm.org/doi/10.1145/3725843.3756071>.
- [35] Varun Rajesh, Om Jodhpurkar, Pooja Anbuselvan, Mantinder Singh, Ashok Jallepali, Shantanu Godbole, Pradeep Kumar Sharma, and Hritvik Shrivastava. Production-grade local llm inference on apple silicon: A comparative study of mlx, mlc-llm, ollama, llama.cpp, and pytorch mps. *arXiv preprint arXiv:2511.05502*, 2025.
- [36] Junyi Wen, Junyuan Liang, Zicong Hong, Wuhui Chen, Ting Cai, and Zibin Zheng. Krul: Efficient state restoration for multi-turn conversations with dynamic cross-layer kv sharing. *arXiv preprint arXiv:2507.08045*, 2025.
- [37] Zunhai Su, Zhe Chen, Wang Shen, Hanyu Wei, Linge Li, Huangqi Yu, and Kehong Yuan. Rotatekv: Accurate and robust 2-bit kv cache quantization for llms via outlier-aware adaptive rotations. In *International Joint Conference on Artificial Intelligence*, 2025. URL <https://arxiv.org/abs/2501.16383>.

A safetensors Q4 Format

The persistent KV cache uses safetensors format with model-specific tensor naming. For a model with L layers, H KV heads, head dimensions D_K and D_V , and N cached tokens:

Tensor schema (per layer l , per block b):

- $L\{1\}_B\{b\}_K.weights$: uint32, shape $(H, D_K/8, 256)$
- $L\{1\}_B\{b\}_K.scales$: bfloat16, shape $(H, D_K, 4)$
- $L\{1\}_B\{b\}_K.biases$: bfloat16, shape $(H, D_K, 4)$
- $L\{1\}_B\{b\}_V.weights$: uint32, shape $(H, D_V/8, 256)$
- $L\{1\}_B\{b\}_V.scales$: bfloat16, shape $(H, D_V, 4)$
- $L\{1\}_B\{b\}_V.biases$: bfloat16, shape $(H, D_V, 4)$

Block size is 256 tokens, group size 64 elements (4 groups per block). For symmetric models (Gemma), $D_K = D_V$. For MLA models (DeepSeek), $D_K = 192$, $D_V = 128$.

Gemma 3’s scales and biases use bfloat16 (preserved natively by MLX’s `mx.save_safetensors`). DeepSeek uses standard float16.

— Supplementary Materials —

B MLX Engineering Notes

MLX uses lazy evaluation: operations build computation graphs that execute only when results are consumed. This creates failure modes when KV cache operations appear to succeed but produce no data.

Table 12: MLX lazy evaluation failure modes relevant to KV cache persistence.

Symptom	Root Cause	Fix
Cache appears empty after prefill	Missing <code>mx.eval()</code> after cache update	Evaluate after update
OOM during batch	Graph accumulates without clearing	Evaluate per iteration
Zeros after disk reload	loaded tensors not evaluated	Evaluate after load
Quantization corruption	Scales/biases lazy	Evaluate quantize output
Attention NaNs	Q4 tensors invalid post-load	Validate dtype/shape
Batch hangs	Merge built graph but not executed	Evaluate before attention

Two additional issues specific to batched inference:

Thread safety. MLX is not thread-safe (GitHub issues #2067, #2133, #3078). Concurrent `mx.eval()` calls from different threads cause Metal assertion failures. We serialize all MLX operations through a single scheduler thread, using an `RLock(mx_io_lock)` to protect cross-thread I/O (cache saves).

mx.compile with variable batch size. `mx.compile` traces shapes at first call and fails on subsequent calls with different batch dimensions. We split batch-2 operations into two batch-1 calls, each through `mx.compile(shapeless=True)`, and concatenate results.

C Benchmark Configuration

Hardware, software, and model specifications are identical to Section 4 (Setup). Additional parameters: Q4 quantization group size 64, prefill chunk size 512 tokens (configurable), scheduler enabled, max batch size 2. 6 passes per configuration with 10–240s adaptive cooldown (thermal-aware with TPS recovery probe). Median values reported.

Measurement counts: Gemma 394 (1K–32K; batch=2 skipped at 32K, 2 hot non-streaming missing). DeepSeek 378 (1K–32K; 32K batch=1 only, 3 passes). Llama 360 (1K–16K). Total: 1,132 measurements.

Measurement ranges (TTFT, ms): Table 13 shows min–max spread across 6 passes for selected configurations (streaming, batch=1).

Table 13: TTFT measurement ranges (ms). Min–median–max of 6 passes.

Model	Cache	1K	4K	16K	32K
Gemma	Cold	3815–3964–4055	15478–15736–16076	74120–74219–74260	171718–172096–172436
	Warm	455–475–539	504–577–608	782–795–817	1748–1819–1921
	Hot	668–683–701	697–719–735	920–934–964	1240–1264–1345
DeepSeek	Cold	1019–1043–1077	3861–3970–4050	19257–19396–19466	47066–47315–47359 [†]
	Warm	227–234–271	263–271–287	407–434–505	631–633–650 [†]
	Hot	323–345–457	352–366–406	483–490–497	614–624–656 [†]
Llama	Cold	2408–2500–2528	10089–10235–10469	45611–47629–48275	—
	Warm	241–260–308	266–290–295	414–431–476	—
	Hot	391–412–430	414–429–446	510–526–537	—

[†]DeepSeek 32K: 3 passes (batch=1 only; memory constraints prevented batch=2 and additional passes).

D FP16 vs Q4 Memory Analysis

Gemma 3 12B (48 layers, 8 KV heads, head dim 256, group size 64):

FP16 per-layer cost = $2 \times 8 \times 256 \times n \times 2$ bytes (K+V, each 2 bytes per element).

At $n = 4096$: $2 \times 8 \times 256 \times 4096 \times 2 = 33,554,432$ bytes = 32 MB per layer \times 48 layers = 1,536 MB.

Q4 per-layer cost: packed 4-bit data = hdn bytes, plus bfloat16 scales and biases = $8hdn/g$ bytes, where $h=8$, $d=256$, $g=64$.

At $n = 4096$: packed data = 8,388,608 bytes (4-bit, half of FP16), scales+biases = 1,048,576 bytes. Total = 9,437,184 bytes = 9.0 MB per layer \times 48 layers = 432 MB.

Ratio: $432/1536 = 0.281$, matching the analytical formula.

DeepSeek-Coder-V2-Lite 16B (27 layers, 16 KV heads, K=192, V=128):

FP16: K cost = $16 \times 192 \times n \times 2$, V cost = $16 \times 128 \times n \times 2$. At $n = 4096$: K = 25,165,824 bytes, V = 16,777,216 bytes. Per layer = 40 MB. \times 27 layers = 1,080 MB.

Q4: same 0.281 ratio applied per tensor. Total = 304 MB.

MoE intermediate tensors add ~ 1 – 2 GB overhead during forward passes, further constraining FP16 capacity. The 4096 MB cache budget for DeepSeek accounts for this.

Llama 3.1 8B (32 layers, 8 KV heads, head dim 128):

FP16 per-layer cost = $2 \times 8 \times 128 \times n \times 2$ bytes. At $n = 4096$: 16,777,216 bytes = 16 MB per layer \times 32 layers = 512 MB. Q4: same 0.281 ratio. Total = 144 MB. Llama’s smaller cache footprint per agent enables 70 agents at 4K Q4 vs 19 in FP16.

E Perplexity Methodology

Section 4.8 reports perplexity measured with actual `QuantizedKVCache` objects. The methodology uses WikiText-2 text in 512-token sliding windows (256-token stride), evaluating 7,935 tokens per model. Both FP16 baseline and Q4 caches use identical model weights (4-bit quantized via `mlx-lm`). The Q4 KV cache uses group size 64, matching the production pipeline.

Table 14: Agent capacity comparison, all models. M4 Pro, 10.2 GB cache budget.

Model	4K		8K		16K		32K	
	FP16	Q4	FP16	Q4	FP16	Q4	FP16	Q4
Gemma 3	6	24	3	12	1	6	0	3
DeepSeek	9	33	4	16	2	8	1	4
Llama 3.1	19	70	9	35	4	17	2	8

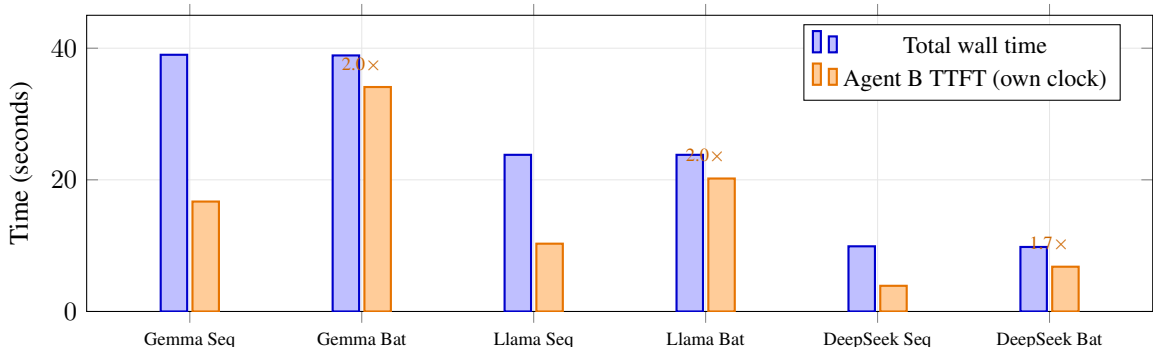


Figure 3: Staggered request arrivals (4K cold context, Agent B arrives 2 s after Agent A). Total wall time is identical between sequential and batched modes. However, Agent B’s own perceived TTFT (submit to first token) is *worse* in batched mode: 34.1 s vs 16.7 s for Gemma (2.0×), 20.2 s vs 10.3 s for Llama (2.0×), 6.8 s vs 3.9 s for DeepSeek (1.7×). In sequential mode, B runs alone with full GPU bandwidth after A completes. In batched mode, B starts 2 s after A but shares prefill bandwidth via interleaved chunking, approximately doubling its individual TTFT.

Prior work on Q4 KV cache quality: KIVI [16] shows negligible downstream task degradation at 4 bits with per-channel key quantization (group 32–64). KVQuant [17] shows <0.1 PPL at 4 bits with per-layer sensitivity calibration. QuantSpec [19] validates 4-bit KV for speculative decoding with no measurable quality loss. RotateKV [37] reports <0.3 PPL **degradation** even at 2 bits. Our Gemma result (−0.7%) is consistent with this literature; our DeepSeek result (+3.0%) is higher, possibly reflecting MLA’s compressed latent representations (Section 4.8).

F Staggered Arrivals

Real multi-agent workflows have staggered request arrivals. A single user may trigger multiple agents in sequence: Agent A begins at $t=0$ (4K cold context), Agent B begins at $t=2s$ (4K cold context).

In sequential mode, Agent B waits for Agent A to complete before starting. In batched mode, Agent B starts 2 s after A and joins A’s batch via interleaved chunked prefill.

Total wall time is identical across all three models: 39.0 s vs 38.9 s (Gemma), 9.9 s vs 9.8 s (DeepSeek), 23.8 s vs 23.8 s (Llama). Agent B’s processing TTFT (from submission to first token) is higher in batched mode because B shares GPU bandwidth during prefill: Gemma 34.1 s batched vs 16.7 s sequential; DeepSeek 6.8 s vs 3.9 s; Llama 20.2 s vs 10.3 s. However, the metric that matters for user responsiveness is *time from desired start to first token*. In sequential mode, B cannot submit until A finishes, adding A’s full end-to-end latency as queue time. In batched mode, B submits immediately and begins processing concurrently. For Gemma, B’s wall-clock wait (desired start to first token) is 36.1 s batched vs 36.5 s sequential—effectively identical, but in the batched case B is *actively being processed* the entire time rather than sitting in a queue. For DeepSeek, 8.8 s vs 8.9 s. For Llama, 22.3 s vs 22.2 s. As context grows, the queue penalty in sequential mode grows quadratically (matching cold TTFT), while batched mode’s concurrent processing keeps B responsive. System throughput is marginally higher in batched mode (DeepSeek: 13.1 vs 12.9 TPS; Llama: 5.4 vs 5.3 TPS). The benefit compounds with warm or hot caches: queue time in sequential mode remains A’s full E2E, but in batched mode both agents complete decode concurrently, making batch=2 strictly better for multi-agent responsiveness.

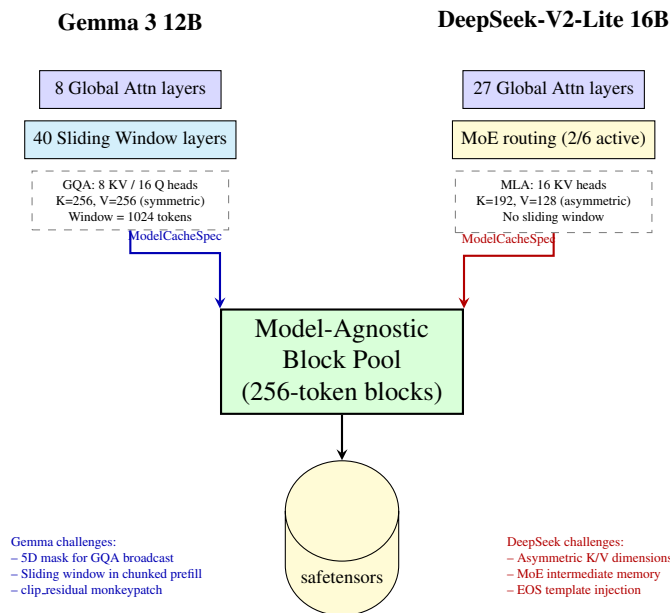


Figure 4: Architecture comparison. The block pool abstracts away architectural differences through ModelCacheSpec. Gemma 3 uses grouped-query attention with hybrid sliding-window layers, requiring 5D mask expansion and window-aware chunked prefill. DeepSeek uses multi-latent attention with asymmetric K/V dimensions (192 vs 128) and MoE routing, requiring larger memory budgets for intermediate tensors.

G Hardware Landscape

All results in this paper are from a single device: Apple MacBook Pro M4 Pro (24 GB, 273 GB/s). This represents the lower end of capable edge devices. The M4 Max (128 GB, 546 GB/s) would fit ~ 134 agents at 8K Q4 context (113 GB available for cache / 0.84 GB per agent = 134.5) vs 12 on the M4 Pro. NVIDIA’s DGX Spark (128 GB, 273 GB/s) matches the M4 Pro’s bandwidth at $5\times$ the memory. Discrete GPU devices (RTX 5090, 32 GB VRAM at 1,792 GB/s) have higher compute bandwidth but spilling KV cache to host RAM drops to PCIe speeds ($28\times$ cliff), making unified memory devices more favorable for cache persistence workflows. Table 1 in the main text summarizes the key specifications.

H Detailed Figures

H.1 Architectural Comparison

Figure 4 compares model architectures. Gemma 3 uses hybrid attention (8 global + 40 sliding window layers) with symmetric KV dimensions. DeepSeek uses MLA with asymmetric dimensions ($K=192$, $V=128$). Llama 3.1 uses standard GQA (32 layers, all global). All three share the same block pool, Q4 pipeline, and BatchQuantizedKVCache via the ModelCacheSpec abstraction.

H.2 Phase Timeline

Figure 5 shows cache state transitions across the 5-phase prisoner’s dilemma scenario. Permanent agents (Warden, Marco, Danny) accumulate warm/hot cache across phases. The ephemeral agent (Analyst) cold-starts in Phase 5 only.

H.3 Wikipedia Routing Diagram

Figure 6 shows the 3-phase routing protocol. Phase 1 primes 10 experts with cold-start prefill. Phase 2 routes cross-topic queries to 2–3 warm experts each. Phase 3 re-queries hot experts.

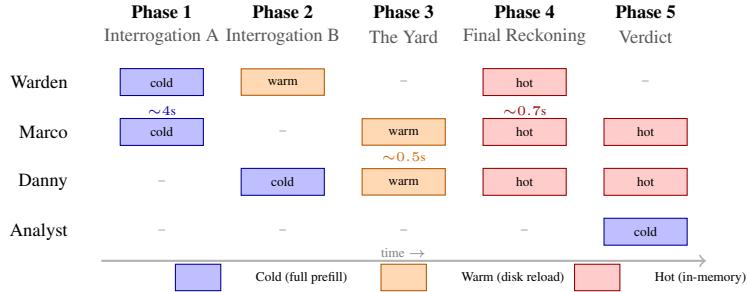


Figure 5: Agent cache state across prisoner’s dilemma phases. Permanent agents (Warden, Marco, Danny) start cold and transition to warm/hot as context accumulates via cross-phase injection. Each phase extends the cached prefix rather than re-computing. The Analyst appears only in Phase 5 (cold start). TTFT annotations show projected latency from Table 3 at equivalent context lengths.

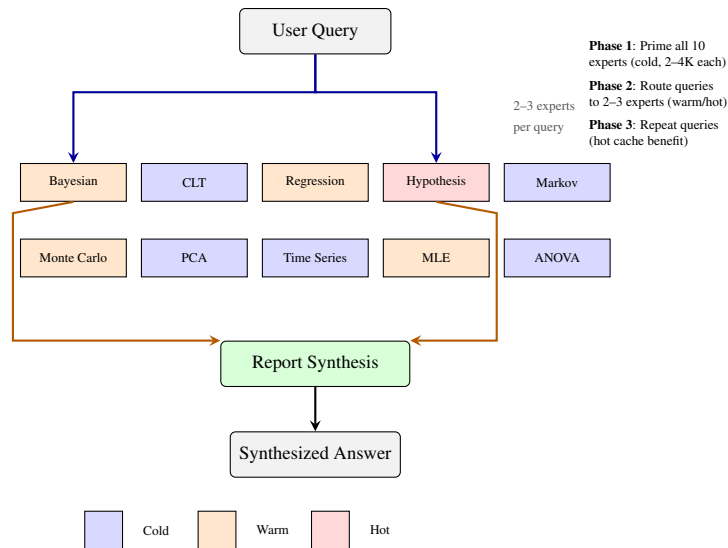


Figure 6: Wikipedia multi-agent routing. Ten expert agents are primed with article content (cold prefill). Cross-topic queries route to 2–3 relevant experts whose caches are warm/hot from priming. A reporter agent synthesizes responses. Repeated queries to the same experts benefit from hot cache (projected 10–30× TTFT reduction vs cold).

I Development Process

This system was developed over 19 days across 44 development sessions, producing 301 commits. The codebase comprises 17.8K lines of source code, 31K lines of tests, and 12.7K lines of benchmark infrastructure.

Benchmarks as tests. The timing benchmarks described in Section 4 served a dual role: they produced the paper’s results *and* functioned as the primary mechanism for discovering bugs. Many of the most consequential bugs (Categories 3 and 4 below) were invisible to unit tests and integration tests but manifested as inconsistent TTFT numbers, unexplained quality regressions, or measurements that contradicted architectural expectations. For example, the batch=2 cache corruption bug (Category 3) was discovered when warm-cache TTFT measurements showed 0-token output in a configuration that should have matched single-request baselines. The sliding window mask bug (Category 4) was caught when perplexity measurements degraded with context length faster than Q4 quantization error alone could explain. In both cases, the fix was confirmed by re-running the full benchmark suite and verifying self-consistency of the numbers. The benchmark infrastructure (12.7K lines) doubles as a testing framework that validates architectural invariants through quantitative observation.

Bug taxonomy. Table 15 categorizes 17 distinct bugs encountered during development into four categories by diagnosis difficulty. The categories reflect a gradient from mechanically fixable (Category 1) to requiring hardware-level observation (Category 4).

Table 15: Bug taxonomy from development. 17 distinct bugs across 135 fix-related commits. Categories ordered by diagnosis difficulty.

Category	Count	Representative Example
1: External dependency	2	Transformers v5.0.0rc1 SentencePiece regression: space markers stripped during decode, all words run together. Fix: <code>pin transformers<5.0.</code>
2: Integration	5	DeepSeek MLA caches K at dim=192 (128+64 rope) but V at dim=128; spec extractor fell back to 128 for both, causing 20% memory undercount. DeepSeek chat template closes <i>every</i> assistant turn with EOS, killing identity injection.
3: Concurrency	6	Batch=2 warm cache produces EOS on first token. Root cause: scheduler thread runs <code>submit()</code> → <code>mx.eval()</code> while event loop runs <code>_save_to_disk()</code> → safetensors save with different locks → SIGSEGV. Initial hypothesis (lazy tensor chain) was wrong; verification script masked the race with sequential timing.
4: Silent correctness	4	Gemma 3 sliding window mask ignored during chunked prefill: <code>QuantizedKVCache.make_mask()</code> returns causal mask regardless of <code>window_size</code> . 40/48 layers get full attention instead of 1024-token window. Output looks plausible; perplexity scaling with context length was the tell.

Categories 1–2 are amenable to AI-assisted diagnosis: the error is visible in output or traceable through documentation. Categories 3–4 require running real code on real hardware in a loop of “run, observe, hypothesize, test, revise.” The first hypothesis for the batch=2 bug was wrong. The sliding window bug produced grammatical, on-topic text that passed casual inspection—only quantitative measurement revealed the corruption.

AI-assisted development. The project used AI pair programming (Claude Code) throughout 44 sessions. Table 16 summarizes the cost breakdown.

Table 16: AI development cost. 44 sessions, 19 days (Jan 22 – Feb 9, 2026). 1,587 human messages, 301 commits.

Model	Input	Output	Cache W	Cache R	Total
Opus 4.5	\$7	\$120	\$908	\$1,225	\$2,260
Sonnet 4.5	\$2	\$50	\$306	\$544	\$902
Opus 4.6	\$2	\$23	\$238	\$522	\$783
Haiku 4.5	\$0	\$0	\$1	\$1	\$2
Total	\$11	\$193	\$1,453	\$2,291	\$3,947

Table 16 reports API-equivalent pricing; the actual out-of-pocket cost was ~\$200 via subscription plan. The API costs reflect what an organization using direct API calls would pay. Cache reads dominate (95% of token volume,

58% of cost). Without prompt caching, the same work would have cost ~\$30,000. The output-to-surviving-code ratio was 11:1 (9.1M tokens generated to produce 800K tokens in the final codebase), reflecting the iterative nature of debugging. AI assistance was most valuable for scaffolding architecture, generating test boilerplate, and fixing Categories 1–2 bugs. For Categories 3–4, the value shifted to code generation after human-driven diagnosis. All code was human-reviewed before commit.